GEOPHYSICS, VOL. 61, NO. 3 (MAY-JUNE 1996); P. 804-814, 7 FIGS.

# Inversion versus migration: A new perspective to an old discussion

C. P. A. Wapenaar*

**ABSTRACT**

Seismic imaging techniques can be subdivided into inversion and migration. The object functions for inversion and migration are, respectively, the medium contrast parameters and reflectivity. In this paper, the relationship between inversion and migration is approached by analyzing the underlying representations (the forward models). It appears that the "two-way representation" (which underlies inversion) as well as the "one-way representation" (which underlies migration) can both be expressed in terms of a volume integral over the appropriate object function. In their linearized form, these representations account for primaries only. In this case, the one-way representation in terms of reflectivity is the most accurate of the two, which implies that proper migration is more accurate than linearized inversion.

Internal multiples can be taken into account by the nonlinear representations. As an alternative, however, the "generalized primary representation" is introduced. In its explicit form, this one-way representation is linear in the reflectivity (opposed to linearized). Nonlinear effects are implicitly accounted for by the generalized primary propagators. The generalized primary representation is a suitable basis for true amplitude migration, taking the angle-dependent dispersive effects of fine layering into account.

## INTRODUCTION

In the literature on acoustical imaging, in general, and on seismic imaging, in particular, one may distinguish between a class of techniques that aims at imaging the medium parameters and another class of techniques in which imaging of the reflectivity is the main goal. In the following, we refer to these classes as (multidimensional) "inversion" and "migration," respectively (This nomenclature is generally used in the geophysical literature. There are, of course, also exceptions. Curiously, in two consecutive papers in **GEOPHYSICS,** Bleistein (1987) uses the term inversion for reflector imaging and Miller et al. (1987) speak of migration for imaging a specific perturbation of the propagation velocity. With all respect for these authors, we take the liberty of referring to Bleistein's reflector imaging as migration and to Miller's velocity imaging as inversion.). Representative papers on inversion include Cohen and Bleistein (1979), Clayton and Stolt (1981), Raz (1981), Bleistein and Cohen (1982), Devaney (1982, 1984), Tarantola (1984) and Wu and Toksöz (1987). Classical references to migration are Claerbout (1971, 1985), Schneider (1978), Stolt (1978), Berkhout and Van Wulfften Palthe (1979), Berkhout (1982), and Hubral (1983). More recent references on true AVA migration are de Bruin et al. (1990) Schleicher et al. (1993), and Beydoun et al. (1994).

For inversion it is common use to define the medium parameters as a superposition of background and perturbation parameters. For a given background medium, inversion thus aims at imaging the contrast between the medium parameters of the actual medium and the background medium. In the following, we will refer to the medium contrast parameters as the "object function" for inversion (a discussion on the determination of the background medium is beyond the scope of this paper). The object function for migration, i.e., reflectivity, is related in a specific manner to the changes of the medium parameters at the boundaries between the different layers. Thus, migration aims at imaging the spatial variations of the parameters of the actual medium.

For a simple two-layer medium, the object functions to be imaged by inversion and migration are illustrated in Figure 1. Note that for this specific configuration the object function for inversion covers the lower half-space whereas the object function for migration is confined to the depth level of the interface. Obviously these object functions are related to each other, hence it is reasonable to assume that inversion and migration are also related. Indeed, in the first half of the 1980s,

Manuscript received by the Editor October 3, 1994; revised manuscript received August 16, 1995.
*Centre for Technical Geoscience, Laboratory of Seismics and Acoustics, Delft University of Technology, P.O. Box 5046, 2600 GA Delft, The Netherlands.

several authors have discussed this relationship. Without claiming completeness, we mention Raz (1981), Bleistein and Cohen (1982), Weglein (1982), Berkhout (1984), Cheng and Coen (1984), and Stolt and Weglein (1985). As an overall conclusion from these papers it is fair to say that "linearized Born inversion" is to a large extent similar to "wave-equation-based depth migration." It is the author's opinion that the choice for either one of these methods should be guided primarily by the type of medium to be imaged and, in close relation to that, by the type of image that one desires. In medical imaging and (to a lesser extent) in nondestrucive testing of construction materials (NDT), the medium may often be seen as a smooth background medium with a distribution of localized inhomogeneities (point-scatterers) superimposed on it. Hence, for these applications inversion is the most appropriate approach. In seismic reflection experiments, on the other hand, the *boundaries* between the different layers are the main cause for scattering. Hence, for seismic imaging, migration appears to be the most logical way to go. Optionally, in an interesting target area the imaged angle-dependent reflectivity can be translated to medium parameters afterward. In this respect, note that at Delft University we regard migration as the nucleus of "seismic inversion in steps" (Berkhout and Wapenaar, 1990, 1993).

In the present paper, we want to approach the discussion on the relationship between inversion and migration from another perspective. Rather than discussing the inversion and migration algorithms themselves, we will discuss the underlying representations of the seismic data (the forward models). First, 'we will briefly review the well known representation that follows from the two-way wave equation for the total wavefield and that expresses the scattered wavefield in terms of a volume integral over the medium contrast parameters. This representation is the basis for inversion. Next, along the same lines, we will derive a representation from a coupled system of one-way wave equations for downgoing and upgoing waves (In the following the coupled system of one-way wave equations for downgoing and upgoing waves will be simply referred to as the one-way wave equation.) It will appear that this one-way representation expresses the scattered wavefield in terms of a volume integral over a contrast'operator. From there onward several approaches can be followed, depending on the choice of the reference operator. The most straightforward choice of the reference operator leads to a contrast operator that will be recognized as a reflection operator. It follows naturally that this reflection operator is proportional to the vertical changes of the actual medium parameters (similar as the reflection function in Figure lc is proportional to the changes of the compression modulus in Figure la). In its linearized form, this one-way representation is the basis for wave-equation-based depth migration, as described in Berkhout (1982). A more complicated choice of the reference operator leads to the so-called 3-D *generalized primary* representation. In this representation, internal multiple scattering is organized quite different in comparison to the usual Neumann or Bremmer series expansions: it is implicitly included in the propagators. In its explicit form, however, the generalized primary representation appears to be *Linear* in the reflection operator (opposed to linearized). This representation is proposed as the basis for a true-amplitude (true AVA) migration scheme that takes the angle-dependent dispersion effects of fine layering into account. This scheme is discussed in detail in a companion paper (Wapenaar and Herrmann, 1996).

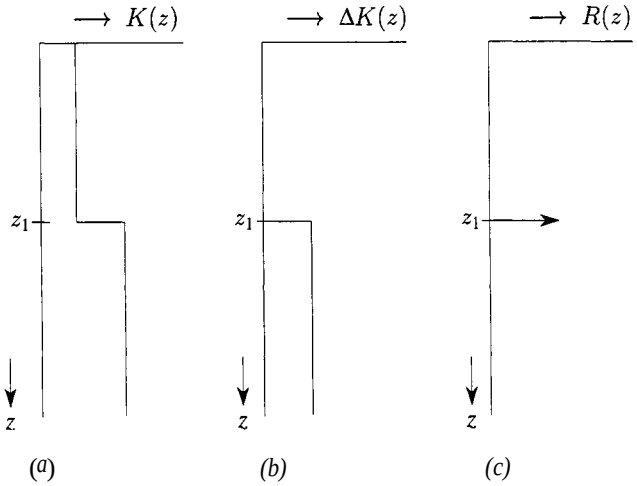


FIG. 1. Illustration of the object functions for inversion and migration for the simple situation of a two-layer medium. (a) Two-layer medium (K is the compression modulus). (b) Object function for inversion. (c) Object function for migration.

## TWO-WAY REPRESENTATIONS

### Nonlinear two-way representation

Consider an inhomogeneous acoustic medium, characterized by the compression modulus K(x) and the mass density $\varrho(\mathbf{x})$, where x is the Cartesian coordinate vector *(x, y, z).* The z-axis is pointing downward. The acoustic pressure in this medium caused by a point source $S(x) = S_o\ (\mathbf{x})\delta(\mathbf{x} - x_s)$ is denoted in the angular frequency domain by P(x). The frequency variable ω is suppressed for notational convenience. Consider a background medium, characterized by $\bar{K}(\mathbf{x})$ and $\bar{\varrho}(\mathbf{x})$. The Green's function in this background medium is denoted by G(x, x'). Moreover, let the medium contrast parameters be denoted by $AK(x) = K(x) - \bar{K}(\mathbf{x})$ and $\Delta\varrho(\mathbf{x}) = p(x) - \bar{\varrho}(\mathbf{x})$. The two-way wave equations for P(x) and G (x, $\mathbf{x}'$) thus read, respectively,

$$\nabla \cdot \left(\frac{1}{\bar{\varrho}} \nabla P\right) + \frac{\omega^2}{\bar{K}} P = -S_{tot}, \tag{1}$$

where

$$S_{tot} = S_0 \delta(\mathbf{x} - \mathbf{x}_S) - \frac{\omega^2 \Delta K}{\bar{K}K} P - \nabla \cdot \left(\frac{\Delta\varrho}{\bar{\varrho}\varrho} \nabla P\right) \tag{2}$$

and

$$\nabla \cdot \left(\frac{1}{\bar{\varrho}} \nabla G\right) + \frac{\omega^2}{\bar{K}} G = -\delta(\mathbf{x} - \mathbf{x}'). \tag{3}$$

In this form, *P(x)* and $G(\mathbf{x}, x')$ satisfy the same wave equation, with different source terms. The two-way representation for the acoustic pressure is thus found by applying the superposition principle, according to

$$P(\mathbf{x}) = \int_{\mathcal{R}^3} G(\mathbf{x}, \mathbf{x}') S_{tot}(\mathbf{x}')\, d^3\mathbf{x}', \tag{4}$$

with $S_{tot}$ given in equation (2) (Morse and Ingard, 1968). Equation (4) is an integral equation of the second kind for P(x). An iterative solution is given by the following Neumann series expansion

$$\{P(\mathbf{x})\}^{(n)} = G(\mathbf{x}, \mathbf{x}_S)S_0(\mathbf{x}_S) + \int_{\mathcal{R}^3} G(\mathbf{x}, \mathbf{x}')\left[\left\{\frac{-\omega^2\Delta K}{\bar{K}K}\right\}(\mathbf{x}')\{P(\mathbf{x}')\}^{(n-1)} - \nabla'\cdot\left(\left\{\frac{\Delta\varrho}{\bar{\varrho}\varrho}\right\}(\mathbf{x}')\nabla'\{P(\mathbf{x}')\}^{(n-1)}\right)\right] d^3\mathbf{x}', \quad (5)$$

for $n > 0$, and $\{P(\mathbf{x})\}^{(0)} = G(\mathbf{x}, \mathbf{x}_S)S_0(\mathbf{x}_S)$.

**Linearized two-way representation**

For $n = 1$, equation (5) reduces to the Born approximation. Applying integration by parts, the term $-G\nabla'\cdot(\{\Delta\varrho/\bar{\varrho}\varrho\}\nabla'P^{(0)})$ may be replaced by $\{\Delta\rho/\bar{\rho}\rho\}\nabla'G\cdot\nabla'P^{(0)}$. Applying a high-frequency approximation to this term yields

$$\{P(\mathbf{x})\}^{(1)} = G(\mathbf{x}, \mathbf{x}_S)S_0(\mathbf{x}_S) + \int_{\mathcal{R}^3} G(\mathbf{x}, \mathbf{x}')\Delta(\mathbf{x}')G(\mathbf{x}', \mathbf{x}_S)S_0(\mathbf{x}_S)\, d^3\mathbf{x}', \quad (6)$$

where the contrast function $\Delta(\mathbf{x}')$ is given by

$$\Delta(\mathbf{x}') = \frac{-\omega^2}{\bar{K}(\mathbf{x}')}\left[\frac{\Delta K(\mathbf{x}')}{K(\mathbf{x}')} + \frac{\Delta\varrho(\mathbf{x}')}{\varrho(\mathbf{x}')}\cos\gamma(\mathbf{x}')\right]. \quad (7)$$

Equation (6) is the two-way representation for primary reflection data. In equation (7), $\gamma(\mathbf{x}')$ is the angle between the rays of $G(\mathbf{x}', \mathbf{x}_S)$ and $G(\mathbf{x}, \mathbf{x}')$ at x'. Interpreting the integral in equation (6) from right to left, one encounters subsequently: propagation from the source at $x_s$ to x', scattering at x' and propagation from x' to the observation point x. This two-way representation is the forward model that underlies linearized Born inversion. We come back to this later on.

## FROM TWO-WAY TO ONE-WAY

At the basis of the one-way representations lies the one-way wave equation, which will be reviewed briefly here. First, consider the two-way wave equation in matrix form

$$\frac{\partial\mathbf{Q}}{\partial z} - \hat{\underline{\mathbf{A}}}\mathbf{Q} = \mathbf{D}, \quad (8)$$

with the two-way wave vector defined as $\mathbf{Q} = (\boldsymbol{P}, \boldsymbol{V_z})^T$, where $\boldsymbol{V_z}$ is the vertical component of the particle velocity. The expressions for the two-way operator matrix $\hat{\underline{\mathbf{A}}}$ and the two-way source vector **D** can be found in many references [see for instance, Kosloff and Baysal (1983) or Wapenaar and Berkhout, (1989, Chapter III)]. The circumflex on $\hat{\mathbf{A}}$ denotes its dependency on the horizontal differentiation operators $\partial/\partial x$ and $\partial/\partial y$. Analogous to the decomposition approach in horizontally layered media [see Ursin, (1983) for an overview], pseudodifferential operator matrices $\hat{\underline{\mathbf{\Lambda}}}$, $\underline{\mathbf{L}}$, and $\hat{\underline{\mathbf{L}}}^{-1}$ can be introduced that satisfy the relation

$$\hat{\underline{\mathbf{A}}} = -j\omega\hat{\underline{\mathbf{L}}}\hat{\underline{\mathbf{\Lambda}}}\hat{\underline{\mathbf{L}}}^{-1}, \quad (9)$$

in such a way that $\hat{\underline{\mathbf{\Lambda}}}$ is diagonal. Assuming that the medium parameters are "sufficiently smooth" this decomposition can be carried out in an exact manner. For an extensive list of references on the theoretical and numerical aspects, see Fishman et al. (1987). Recent references in the seismic context are de Hoop (1992) and Wapenaar and Grimbergen (1996).

Let **P** and S denote a one-way wave vector and a one-way source vector, according to $\mathbf{P} = (\boldsymbol{P}^+, \boldsymbol{P}^-)^T$ and $S = (S^+, S^-)^T$, where $\boldsymbol{P}^+$ and $\boldsymbol{P}^-$ represent (flux normalized) downgoing and upgoing waves, respectively, and where S + and S - represent source functions for downgoing and upgoing waves, respectively. Let these one-way wave and source vectors be related to the two-way wave vectors, according to

$$\mathbf{Q} = \hat{\underline{\mathbf{L}}}\mathbf{P} \text{ and } \mathbf{D} = \hat{\underline{\mathbf{L}}}\mathbf{S}. \quad \mathbf{(10)}$$

Substitution of equations (9) and (10) into the two-way wave equation (8) yields the one-way wave equation

$$\frac{\partial\mathbf{P}}{\partial z} - \hat{\underline{\mathbf{B}}}\mathbf{P} = \mathbf{S}, \quad (11)$$

where the one-way operator matrix $\hat{\underline{\mathbf{B}}}$ is defined as

$$\hat{\underline{\mathbf{B}}} = -j\omega\hat{\underline{\mathbf{\Lambda}}} + \hat{\underline{\mathbf{\Theta}}}, \quad (12)$$

with

$$\hat{\underline{\mathbf{\Theta}}} = -\hat{\underline{\mathbf{L}}}^{-}\frac{\partial\hat{\underline{\mathbf{L}}}}{\partial z}. \quad (13)$$

From the structure of equations (11) through (13), it follows that the diagonal operator matrix $-j\omega\hat{\underline{\mathbf{\Lambda}}}$ explicitly accounts for propagation and $\hat{\underline{\mathbf{\Theta}}}$ for scattering caused by the vertical variations of the medium parameters (both operator matrices also account implicitly for scattering caused by the horizontal variations). In particular, by writing

$$\hat{\underline{\mathbf{\Theta}}} = \begin{pmatrix} \hat{T}^+ & \hat{R}^- \\ -\hat{R}^+ & -\hat{T}^- \end{pmatrix}, \quad (14)$$

$\hat{R}^{\pm}$ and $\hat{T}^{\pm}$ are recognized as the reflection and transmission operators for downgoing and upgoing waves [the + and - signs in equation (14) are chosen for later convenience].

The explicit distinction between propagation and scattering is an important advantage of the one-way wave equation (11) over the two-way wave equation (8). This property is exploited in this paper in the derivation of the one-way primary representation and the one-way ***generalized*** primary representation.

## ONE-WAY REPRESENTATIONS

**Nonlinear one-way representation**

Let **P(x)** denote the one-way wavefield caused by a one-way point source $S(x) = S_o(\mathbf{x})\delta(\mathbf{x} - x_s)$. Consider a reference operator $\bar{\underline{\mathbf{B}}}(\mathbf{x})$ that governs a one-way Green's matrix $\underline{\mathbf{G}}(\mathbf{x}, x')$. Moreover, let the contrast operator be denoted by $\hat{A}(x) = \hat{\underline{\mathbf{B}}}(\mathbf{x}) - \bar{\underline{\mathbf{B}}}(\mathbf{x})$. The one-way wave equations for **P(x)** and $\underline{\mathbf{G}}(\mathbf{x}, x')$ thus read, respectively,

$$\frac{\partial\mathbf{P}}{\partial z} - \hat{\bar{\underline{\mathbf{B}}}}\mathbf{P} = \mathbf{S}_{tot}, \quad (15)$$

where

$$\mathbf{S}_{tot} = \mathbf{S}_0\delta(\mathbf{x} - \mathbf{x}_S) + \hat{\underline{\Delta}}\mathbf{P} \tag{16}$$

and

$$\frac{\partial \underline{\mathbf{G}}}{\partial z} - \hat{\underline{\mathbf{B}}}\underline{\mathbf{G}} = \underline{\mathbf{I}}\delta(\mathbf{x} - \mathbf{x}'). \tag{17}$$

The Green's matrix $\underline{\mathbf{G}}(\mathbf{x}, \mathbf{x}')$ has the following structure

$$\underline{\mathbf{G}}(\mathbf{x}, \mathbf{x}') = \begin{pmatrix} G^{+,+}(\mathbf{x}, \mathbf{x}') & G^{+,-}(\mathbf{x}, \mathbf{x}') \\ G^{-,+}(\mathbf{x}, \mathbf{x}') & G^{-,-}(\mathbf{x}, \mathbf{x}') \end{pmatrix}, \tag{18}$$

where the superscripts refer to the propagation direction at x and x', respectively. $\mathbf{P(x)}$ and $\underline{\mathbf{G}}(\mathbf{x}, \mathbf{x}')$ satisfy the same wave equation, with different source terms. The one-way representation for the one-way wave vector $\mathbf{P(x)}$ is thus found by applying the superposition principle, according to

$$\mathbf{P}(\mathbf{x}) = \int_{\mathcal{R}^3} \underline{\mathbf{G}}(\mathbf{x}, \mathbf{x}')\mathbf{S}_{tot}(\mathbf{x}')\, d^3\mathbf{x}', \tag{19}$$

with $S_{tot}$ given in equation (16). Equation (19) is an integral equation of the second kind for $\mathbf{P(x)}$. An iterative solution is given by the following Neumann series expansion

$$\{\mathbf{P}(\mathbf{x})\}^{(n)} = \underline{\mathbf{G}}(\mathbf{x}, \mathbf{x}_S)\mathbf{S}_0(\mathbf{x}_S) + \int_{\mathcal{R}^3} \underline{\mathbf{G}}(\mathbf{x}, \mathbf{x}')\hat{\underline{\Delta}}(\mathbf{x}')\{\mathbf{P}(\mathbf{x}')\}^{(n-1)}\, d^3\mathbf{x}', \tag{20}$$

for $n > 0$, and $\{\mathbf{P}(\mathbf{x})\}^{(0)} = \underline{\mathbf{G}}(\mathbf{x}, \mathbf{x}_S)\mathbf{S}_0(\mathbf{x}_S)$.

### Linearized one-way representation

Choosing $n = 1$ in equation (20) yields

$$\{\mathbf{P}(\mathbf{x})\}^{(1)} = \underline{\mathbf{G}}(\mathbf{x}, \mathbf{x}_S)\mathbf{S}_0(\mathbf{x}_S) + \int_{\mathcal{R}^3} \underline{\mathbf{G}}(\mathbf{x}, \mathbf{x}')\hat{\underline{\Delta}}(\mathbf{x}')\underline{\mathbf{G}}(\mathbf{x}', \mathbf{x}_S)\mathbf{S}_0(\mathbf{x}_S)\, d^3\mathbf{x}', \tag{21}$$

with $\hat{\underline{\Delta}} = \hat{\underline{\mathbf{B}}} - \hat{\underline{\mathbf{B}}}$. In analogy with equation (12), the reference operator $\hat{\underline{\mathbf{B}}}$ is defined as $\hat{\underline{\mathbf{B}}} = -j\omega\hat{\underline{\Delta}} + \hat{\underline{\Theta}}$. This operator allows an independent choice of $\hat{\underline{\Delta}}$ (propagation) and $\hat{\underline{\Theta}}$ (scattering). For the moment we choose

$$\hat{\underline{\Delta}} = \hat{\underline{\Delta}} \quad \text{(propagation in the actual medium)} \tag{22}$$

and

$$\hat{\underline{\Theta}} = \underline{\mathbf{O}} \quad \text{(no scattering; } \underline{\mathbf{O}} \text{ is the null matrix)}. \tag{23}$$

As a consequence, the reference operator, $\hat{\underline{\mathbf{B}}} = -j\omega\hat{\underline{\Delta}}$, accounts for *primary* propagation in the *actual* medium. Substituting this diagonal reference operator into equation (17) and choosing the appropriate boundary conditions (i.e., outgoing waves for $z \to -\infty$ and for $z \to \infty$), it follows that the Green's primary matrix, which we denote by $\underline{\mathbf{G}}_p(\mathbf{x}, \mathbf{x}')$, has a diagonal form as well. In particular,

$$\underline{\mathbf{G}}_p(\mathbf{x}, \mathbf{x}') = \begin{pmatrix} 0 & 0 \\ 0 & -W_p^-(\mathbf{x}, \mathbf{x}') \end{pmatrix}, \quad \text{for } z' > z, \tag{24}$$

with $W_p^-(\mathbf{x}, \mathbf{x}') \overset{\text{def}}{=} -G_p^{-,-}(\mathbf{x}, \mathbf{x}')$ and

$$\underline{\mathbf{G}}_p(\mathbf{x}', \mathbf{x}_S) = \begin{pmatrix} W_p^+(\mathbf{x}', \mathbf{x}_S) & 0 \\ 0 & 0 \end{pmatrix}, \quad \text{for } z' > z_S, \tag{25}$$

with $W_p^+(\mathbf{x}', \mathbf{x}_S) \overset{\text{def}}{=} G_p^{+,+}(\mathbf{x}', \mathbf{x}_S)$ (the + and - signs are chosen for later convenience). $W_p^+$ (x', $x_s$) and $Wi$ (x, x') will be referred to as the propagators for the primary downgoing and upgoing waves in the actual medium. It can be shown that $W_p^-(\mathbf{x}, \mathbf{x}') = W_p^+$ (x', x) (Wapenaar, 1996).

Another consequence of the choices introduced in equations (22) and (23) is that the contrast operator, $\hat{\underline{\Delta}} = \hat{\underline{\mathbf{B}}} - \hat{\underline{\mathbf{B}}}$, appears to be identical to the scattering operator $\hat{\underline{\Theta}}$ of the actual medium. Hence,

$$\hat{\underline{\Delta}}(\mathbf{x}') = \hat{\underline{\Theta}}(\mathbf{x}') = \begin{pmatrix} \hat{T}^+(\mathbf{x}') & \hat{R}^-(\mathbf{x}') \\ -\hat{R}^+(\mathbf{x}') & -\hat{T}^-(\mathbf{x}') \end{pmatrix}. \tag{26}$$

Finally, consider a configuration in which the upper half-space $z \le z_0$ is homogeneous and choose $x_s$ and x in this upper half-space. In particular, consider the primary upgoing response $\{P - (x)\}^{(1)}$ related to the source function $S_0^+$ (xs ) for downgoing waves and choose $S_0^-$ ( $x_s$ ) = 0. Upon substitution of equations (24), (25), and (26) into equation (21), one thus obtains for the lower element in $\{\mathbf{P(x)}\}^{(1)}$

$$\{P^-(\mathbf{x})\}^{(1)} = \int_{\Omega} W_p^-(\mathbf{x}, \mathbf{x}')\hat{R}^+(\mathbf{x}')\, W_p^+(\mathbf{x}', \mathbf{x}_S)S_0^+(\mathbf{x}_S)\, d^3\mathbf{x}', \tag{27}$$

where $\Omega$ denotes the lower half-space $z' > z_0$ . Equation (27) is the one-way representation for primary reflection data. From right to left, one subsequently encounters: downward propagation from the source at $x_s$ to x', reflection at x', and upward propagation from x' to the observation point x. This one-way representation was introduced (in a discrete formulation) in Berkhout (1982) for acoustic one-way wavefields in fluids and modified in Wapenaar and Berkhout (1989) for elastodynamic one-way wavefields in solids. It is the forward model that underlies wave-equation-based depth migration.

## COMPARISON OF THE LINEARIZED IMAGING APPROACHES

In this section we compare linearized Born inversion and wave-equation-based depth migration.

**Linearized Born inversion.**-Given the measured wavefield $P(x) \approx \{P(x)\}^{(1)}$, the source $S_o$ ($x_s$) and the Green's functions G( x', $x_s$) and G(x, x') in the background medium, linearized Born inversion aims at imaging the contrast function $\Delta(\mathbf{x}')$ by inverting equation (6).

**Wave equation based depth migration.-Given** the upgoing wavefield $P$ - (x) $\approx$ {P - (x) } $^{(1)}$, the downgoing source $S_0^+$ ($x_s$) and the primary propagators $W_p^+$ (x', $x_s$) and $W_p^-$ **(x, x')** in the actual medium, wave-equation-based depth migration aims at imaging the reflection operator $\hat{R}^+$ (x') by inverting equation (27). Note that in practice most migration schemes only image a reflection coefficient $R^+$ (x'). Imaging the reflection operator $\hat{R}^+$ (x') is equivalent with imaging an angle-dependent reflection coefficient $R^+$ (x', a) (Berkhout and Wapenaar, 1993).

The similarity between both approaches is obvious; here we want to discuss some differences.

**Scattering.**- The contrast function in the two-way representation describes the difference between the medium parameters of the actual medium and the background medium; the reflection operator in the one-way representation is proportional to the vertical variations of the actual medium parameters. This distinction was already mentioned in the introduction and was illustrated for a two-layer medium in Figure 1. For this same medium it can be shown that the linearized one-way representation (27) is exact (bear in mind that no multiple scattering occurs), whereas the linearized two-way representation (6) involves an approximation. As a consequence, wave-equation- based depth migration may handle the amplitudes more accurately than linearized Born inversion.

**Propagation.**- The Green's functions in the two-way representation are defined in the background medium, whereas the propagators in the one-way representation are defined in the actual medium. In the practice of wave-equation-based depth migration, these propagators are defined in a *macro model,* which accounts for the traveltimes as accurately as possible. Note the subtle difference with the background medium, used for inversion: a background medium is by definition different from the actual medium, hence, the traveltimes of the Green's functions will generally have a bias. In practice, however, this difference between the background medium and the macro model is of minor importance in comparison to the errors involved both in background and macro model estimation.

Hence, the main advantage of wave-equation-based depth migration is that it handles the amplitudes more accurately than linearized Born inversion. Of course, this is only true when the propagators $W_p^+$ and $W_p^-$ and their inverse versions are properly computed. Note that these inverse versions are simply obtained by complex conjugation of the forward propagators. This applies to homogeneous as well as to moderately inhomogeneous macro models (Berkhout, 1982; Wapenaar and Berkhout, 1989).

## THE GENERALIZED PRIMARY REPRESENTATION

The nonlinear two-way representation (5) as well as its one-way counterpart (20) both account for multiple scattering. In particular, upon substitution of $\hat{\underline{\Delta}} = \hat{\underline{\Theta}}$ and $\underline{G} = \underline{G}_p$ in the one-way Neumann series (20), one obtains a generalized Bremmer series, according to

$$\{\mathbf{P}(\mathbf{x})\}^{(n)} = \underline{G}_p(\mathbf{x}, \mathbf{x}_S)\mathbf{S}_0(\mathbf{x}_S) + \int_{\mathcal{R}^3} \underline{G}_p(\mathbf{x}, \mathbf{x}')\hat{\underline{\Theta}}(\mathbf{x}')\{\mathbf{P}(\mathbf{x}')\}^{(n-1)}\, d^3\mathbf{x}', \quad (28)$$

for $n > 0$, and $\{\mathbf{P}(\mathbf{x})\}^{(0)} = \underline{G}_p(\mathbf{x}, \mathbf{x}_S)\,\mathbf{S}_0(\mathbf{x}_S)$. This is a generalization (for laterally variant media) of the "geometrical optics" approach for laterally invariant media (Brekhovskikh, 1960). The main property of a Bremmer series is that each term fully accounts for one order of multiple reflections. For further discussion, see Corones (1975) and de Hoop (1992).

Here, we follow a completely different approach that also accounts for multiple scattering and that exploits the natural distinction between propagation and scattering in the one-way reference operator $\hat{\underline{\mathbf{B}}} = -j\omega\hat{\underline{\Delta}} + \hat{\underline{\Theta}}$. This time we choose

$$\hat{\underline{\Delta}} = \hat{\underline{\Delta}} \quad \text{(propagation in the actual medium)} \quad (29)$$

and

$$\hat{\underline{\Theta}} = H(\zeta - z)\hat{\underline{\Theta}} \quad \text{(scattering only for } z < \zeta), \quad (30)$$

where $H(z)$ is the Heaviside step function and $\zeta$ denotes an arbitrary depth level. Thus, for the reference operator we write

$$\hat{\underline{\mathbf{B}}}(\mathbf{x}|\zeta) = -j\omega\hat{\underline{\Delta}}(\mathbf{x}) + H(\zeta - z)\hat{\underline{\Theta}}(\mathbf{x}). \quad (31)$$

Hence, for a given value of $\zeta$, $\hat{\underline{\mathbf{B}}}(\mathbf{x}|\zeta)$ applies to a configuration that is identical to the actual medium in the upper half-space $z < \zeta$ and that is scatter-free (i.e., no scattering along the z-axis) in the lower half-space $z > \zeta$. Let $\bar{\underline{\mathbf{B}}}(\mathbf{x}|\zeta)$ govern a Green's matrix $\underline{G}(\mathbf{x}, \mathbf{x}'|\zeta)$, as in equation (17), and let a similar operator $\bar{\underline{\mathbf{B}}}(\mathbf{x}|\xi)$ govern a reference wave vector $\bar{\mathbf{P}}(\mathbf{x}|\xi)$, as in equation (11). Note that $\bar{\mathbf{P}}(\mathbf{x}|\infty) = \mathbf{P}(\mathbf{x})$ and $\bar{\mathbf{P}}(\mathbf{x}|-\infty) = \underline{G}_p(\mathbf{x}, \mathbf{x}_S)\,\mathbf{S}_0(\mathbf{x}_S)$. Following the same procedure as before, one obtains instead of equation (19)

$$\bar{\mathbf{P}}(\mathbf{x}|\xi) = \int_{\mathcal{R}^3} \underline{G}(\mathbf{x}, \mathbf{x}'|\zeta)\,\underbrace{\{\mathbf{S}_0(\mathbf{x}')\delta(\mathbf{x}' - \mathbf{x}_S) + \hat{\underline{\Delta}}(\mathbf{x}')\bar{\mathbf{P}}(\mathbf{x}'|\xi)\}}_{\mathbf{S}_{tot}(\mathbf{x}')}\, d^3\mathbf{x}', \quad (32)$$

or

$$\bar{\mathbf{P}}(\mathbf{x}|\xi) - \bar{\mathbf{P}}(\mathbf{x}|\zeta) = \int_{\mathcal{R}^3} \underline{G}(\mathbf{x}, \mathbf{x}'|\zeta)\,\underbrace{\{\hat{\underline{\mathbf{B}}}(\mathbf{x}'|\xi) - \hat{\underline{\mathbf{B}}}(\mathbf{x}'|\zeta)\}}_{\hat{\underline{\Delta}}(\mathbf{x}')}\,\bar{\mathbf{P}}(\mathbf{x}'|\xi)\, d^3\mathbf{x}', \quad (33)$$

where

$$\bar{\mathbf{P}}(\mathbf{x}|\zeta) = \underline{G}(\mathbf{x}, \mathbf{x}_S|\zeta)\mathbf{S}_0(\mathbf{x}_S). \quad (34)$$

Next, choose $\xi = \zeta + d\zeta$, divide both sides of equation (33) by $d\zeta$, and take the limit for $d\zeta \to 0$. This yields

$$\frac{\partial\bar{\mathbf{P}}(\mathbf{x}|\zeta)}{\partial\zeta} = \int_{\mathcal{R}^3} \underline{G}(\mathbf{x}, \mathbf{x}'|\zeta)\frac{\partial\hat{\underline{\mathbf{B}}}(\mathbf{x}'|\zeta)}{\partial\zeta}\bar{\mathbf{P}}(\mathbf{x}'|\zeta)\, d^3\mathbf{x}', \quad (35)$$

where, according to equation (31),

$$\frac{\partial\hat{\underline{\mathbf{B}}}(\mathbf{x}'|\zeta)}{\partial\zeta} = \delta(\zeta - z')\hat{\underline{\Theta}}(\mathbf{x}'). \quad (36)$$

Substituting equation (36) into (35) and replacing $\zeta$ by $z'$ in the result yields

$$\frac{\partial\bar{\mathbf{P}}(\mathbf{x}|z')}{\partial z'} = \int_{\mathcal{R}^2} \underline{G}(\mathbf{x}, \mathbf{x}'|z')\hat{\underline{\Theta}}(\mathbf{x}')\bar{\mathbf{P}}(\mathbf{x}'|z')\, d^2\mathbf{x}'_H, \quad (37)$$

where $\mathbf{x}'_H = (x', y')$. Integrating both sides with respect to $z'$ from -- to $\infty$, using $\bar{\mathbf{P}}(\mathbf{x}|\infty) = \mathbf{P}(\mathbf{x})$ and $\bar{\mathbf{P}}(\mathbf{x}|-\infty) = \underline{G}_p(\mathbf{x}, \mathbf{x}_S)\mathbf{S}_0(\mathbf{x}_S)$, yields

$$\mathbf{P}(\mathbf{x}) = \underline{\mathbf{G}}_p(\mathbf{x}, \mathbf{x}_S)\mathbf{S}_0(\mathbf{x}_S) + \int_{\mathcal{R}^3} \underline{\mathbf{G}}(\mathbf{x}, \mathbf{x}'|z')\hat{\underline{\Theta}}(\mathbf{x}')\bar{\mathbf{P}}(\mathbf{x}'|z')\, d^3\mathbf{x}', \quad (38)$$

where

$$\bar{\mathbf{P}}(\mathbf{x}'|z') = \underline{\mathbf{G}}(\mathbf{x}', \mathbf{x}_S|z')\mathbf{S}_0(\mathbf{x}_S). \quad (39)$$

Note that the structure of equation (38) very much resembles the structure of the Bremmer series expansion (28). However, multiple scattering is organized quite differently. In equations (38) and (39) the multiple scattering effects are fully included in the Green's matrices $\underline{\mathbf{G}}(\mathbf{x}, \mathbf{x}'|z')$ and $\underline{\mathbf{G}}(\mathbf{x}', \mathbf{x}_S|z')$. Hence, implicitly equations (38) and (39) are nonlinear in the scattering operator $\hat{\underline{\Theta}}(\mathbf{x}')$. However, in its explicit form, the system of equations (38) and (39) is *linear* in $\underline{\Theta}(\mathbf{x}')$ (opposed to linearized). We will come back to this later.

In the following, we apply this representation to the configuration of Figure 2, in which the upper half-space $z \leq z0$ is homogeneous. Moreover, we choose xs and x in this upper half-space. The general structure of the Green's matrices is the same as in equation (18). With the appropriate boundary conditions (i.e., outgoing waves for $z \to -\infty$ and for $z \to \infty$) it follows that

$$\underline{\mathbf{G}}(\mathbf{x}, \mathbf{x}'|z') = \begin{pmatrix} 0 & 0 \\ 0 & -W_g^-(\mathbf{x}, \mathbf{x}') \end{pmatrix}, \quad \text{for} \quad z' > z_0 \geq z, \quad (40)$$

with $W_g^-(\mathbf{x}, \mathbf{x}') \overset{\text{def}}{=} -G^{-,-}(\mathbf{x}, \mathbf{x}'|z')$ and

$$\underline{\mathbf{G}}(\mathbf{x}', \mathbf{x}_S|z') = \begin{pmatrix} W_g^+(\mathbf{x}', \mathbf{x}_S) & 0 \\ 0 & 0 \end{pmatrix}, \quad \text{for} \quad z' > z_0 \geq z_S, \quad (41)$$

with $W_g^+(\mathbf{x}', \mathbf{x}_S) \overset{\text{def}}{=} G^{+,+}(\mathbf{x}', \mathbf{x}_S|z')$ (remember that for $\underline{\mathbf{G}}$ the half-spaces above $z_0$ as well as below z' are scatter-free (see Figure 2) so the antidiagonal elements are zero again). $W_g^+(\mathbf{x}', \mathbf{x}_S)$ and $W_g^-(\mathbf{x}, \mathbf{x}')$ will be referred to as the propagators for the *generalized primary* downgoing and upgoing waves, respectively. It can be shown that $W_g^-(\mathbf{x}, \mathbf{x}') = W_g^+(\mathbf{x}', \mathbf{x})$ (Wapenaar, 1996). These propagators play the same role in equations (40) and (41) as the primary propagators in equations (24) and (25), but they include multiple scattering in the region between *z0* and z', hence the name "generalized primary." Hubral et al. (1980) and Resnick et al. (1986) used the same term for the equivalent situation in laterally invariant media. Finally, consider again the special situation for which $S_0^-(\mathrm{xS}) = 0$. In a similar way as before, for the lower element in **P(x)** we obtain

$$P^-(\mathbf{x}) = \int_\Omega W_g^-(\mathbf{x}, \mathbf{x}')\hat{R}^+(\mathbf{x}')W_g^+(\mathbf{x}', \mathbf{x}_S)S_0^+(\mathbf{x}_S)\, d^3\mathbf{x}', \quad (42)$$

see Figure 2 again. This generalized primary representation has the same form as the primary representation (27), but it includes all multiple scattering in the lower half-space.

The representations (38) and (42) in itself are exact. Of course in practice approximations must be made. For instance, the Green's matrix $\underline{\mathbf{G}}$ (and hence the propagators $W_g^{\pm}$) could be approximated by a truncated Bremmer series, analogous to equation (28) (Wapenaar, 1996, Appendix B). Alternatively, we can look upon equation (42) as a starting point for an efficient *parameterization* of the reflection response. We come back to this in the next section.

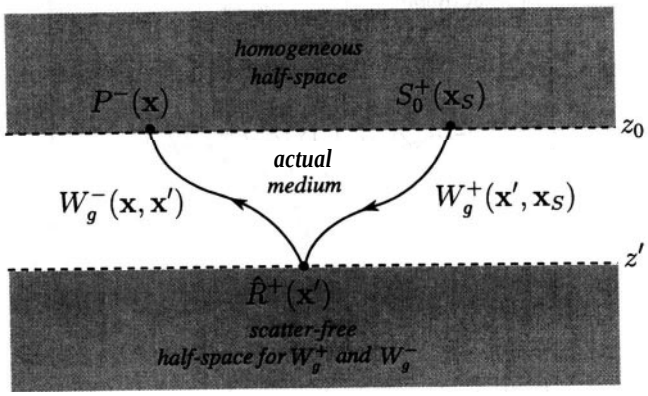


FIG. 2. Configuration for the generalized primary re resentation. $W^+(\mathbf{x}', \mathbf{x}_S)$ and $W_g^-(\mathbf{x}, \mathbf{x}')$ are defined in the actual medium between *z0* and z' and a "scatter-free" half-space below **z' . P** - (x) is the response of the actual medium.

## ACCOUNTING FOR FINE LAYERING

In inversion as well as in migration, it is common to ignore the rapid spatial variations of the medium parameters at a scale smaller to much smaller than the seismic wavelength (fine layering). This is understandable, since the resolving power of any imaging technique is limited to details in the order of half the wavelength. It is not the intention of this paper to circumvent this resolution limit and image the small scale variations. However, it has been recognized by many researchers that these small scale variations may seriously affect the *propagation* properties of the seismic wavefield. In particular, in the last three decades much research has been done on wave propagation through 1-D finely layered media. These studies have shown that the small scale variations manifest themselves as an apparent anisotropic dispersion of the seismic wavefield. Hence, ignoring these variations in inversion or migration implies that AVA effects are not handled properly. In this section, we analyze, *qualitatively*, to what extent the different representations discussed above account for fine layering, and we indicate the implications for inversion and migration. (Throughout this paper we use the term "fine layering" as an equivalent for "small scale variations," because in seismics it refers to the most significant small scale variations. Hence, note that in this paper fine layering is not restricted to 1-D media.)

### Linearized two-way representation

Consider the linearized two-way representation (6) (i.e., the Born approximation), applied to a scattering volume V with limited dimensions and choose the source at $x_s$ and the detector at x both outside this volume. The following is a qualitative analysis, so for convenience we choose a homogeneous background medium with propagation velocity $\bar{c} = \sqrt{\bar{K}/\bar{\rho}}$. Moreover, we assume $\Delta\rho = 0$, so that $\Delta(\mathbf{x}')$ does not depend on the angle $\gamma$. Let i\(k) denote the 3-D spatial Fourier

transform of $\Delta(\mathbf{x}')$. When the source and detector are in the far-field of the scattering volume, so that the Green's functions may be replaced by their Fraunhofer approximations for all x' in V, then the integral in equation (6) appears to be proportional to $\check{\Delta}(\mathbf{k}_D - \mathbf{k}_S)$ (Wolf, 1969; Devaney, 1982,1984). Here $k_s$ and $k_D$ are wave vectors pointing, respectively, from the source to the center of the scattering volume and from this center to the detector. In Figure 3 the total shaded area (dark and light) represents the Fourier transformed contrast function i\(k). The dark shaded sphere denotes the area that is occupied by $\check{\Delta}(\mathbf{k}_D - \mathbf{k}_S)$ for all possible values of $k_D$ and $k_s$ in case of a complete acquisition around the scattering volume (i.e., reflection and transmission measurements). The radius of this sphere is given by $2\omega_{max}/\bar{c}$, where $\omega_{max}$ is the maximum frequency of the source. In practical situations (reflection measurements only; limited aperture), only a part of this sphere is occupied by $\check{\Delta}(\mathbf{k}_D$ - $k_s)$. The point here, however, is that the entire area outside the sphere is not occupied by $\Delta(\mathbf{k}_D$ - $k_s)$ and thus does not contribute to $\{P(\mathbf{x})\}^{(1)}$. In other words, the linearized two-way representation does *not* account for the small scale variations of $\Delta(\mathbf{x}')$, represented by the light shaded area in Figure 3. The consequences for Born inversion are two-fold:

1) Born inversion cannot resolve the small scale variations of $\Delta(\mathbf{x}')$, represented by the light shaded area in Figure 3 (this is almost trivial, but it is stated here for completeness).
2) Born inversion erroneously resolves the intermediate and large-scale variations of $\Delta(\mathbf{x}')$, represented by the dark shaded sphere in Figure 3. In particular, the image will be dispersed, since the linearized two-way representation does not account for the dispersive propagation effects related to the small scale variations of $\Delta(\mathbf{x}')$.

The latter aspect is illustrated in Figure 4 for a 1-D experiment, i.e., a vertically propagating plane-wave in a laterally invariant medium. Figure 4a represents the propagation velocity c as a function of depth *z*. It is a periodically varying function (fine layering), superposed on a step function.

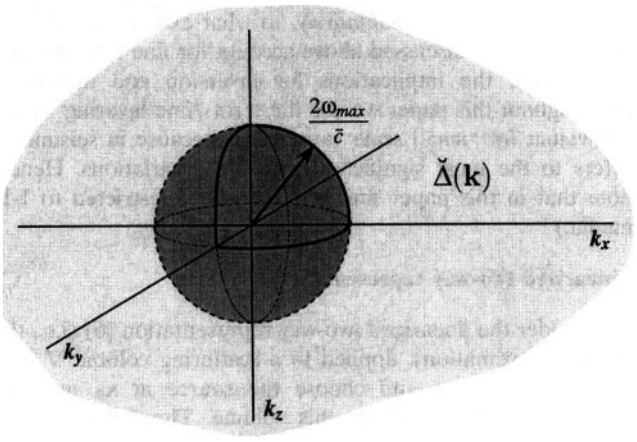


FIG. 3. Spatially Fourier transformed contrast function. The light shaded area, representative for the fine layering, does *not* contribute to the scattered wavefield, as described by the linearized two-way representation.

The background velocity $\bar{c}$ is chosen such that the two-way primary traveltime $t_{prim}$ between $z_0$ = 0 m and the step at $z_1$ = 1000 m is the same in the background medium as in the actual medium (hence, $\bar{c}$ = *(s(z))* $^{-1}$, where (s(z)) is the slowness, averaged over the indicated depth interval). Figure 4b shows the Fourier transform $\check{\Delta}'(k_z)$ of the derivative of the contrast function (the derivative has been taken for display purposes). It may be seen as a 1-D cross-section (along the positive $k_z$ -axis) of Figure 3. The spike corresponds to the

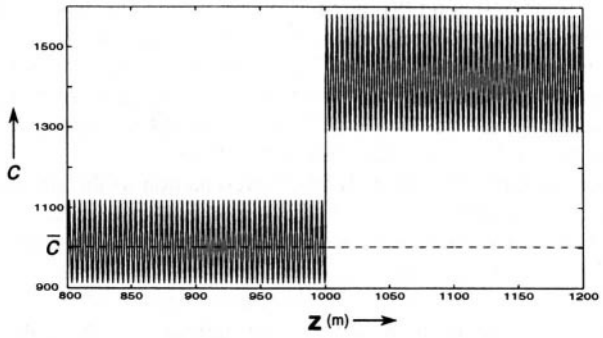


(a)

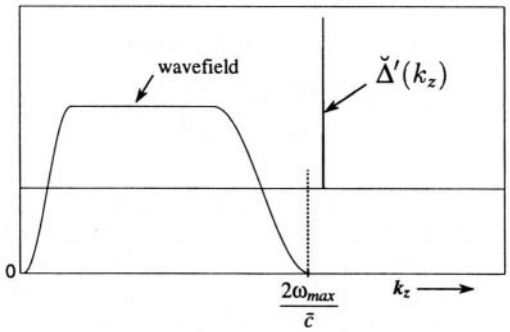


(b)

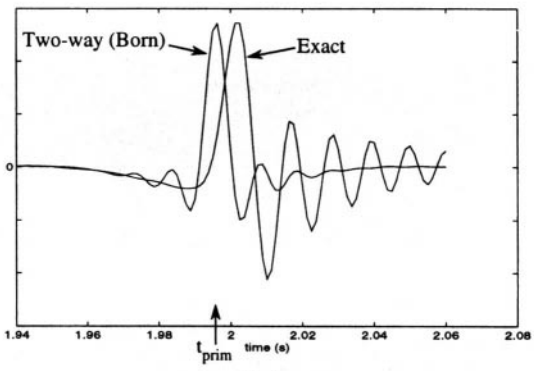


(c)

FIG. 4. 1-D illustration of the linearized two-way representation (Born approximation). (a) Propagation velocity *c( z):* step function + fine layering. (b) Spatial Fourier transform of the derivative of the contrast function. (c) Reflection response according to the linearized two-way representation.

periodic variations in Figure 4a, and the constant (i.e., $k_z$-independent) level corresponds to the derivative of the step in Figure 4a. The spectrum of the source, scaled by $2/\bar{c}$, is also shown in Figure 4b. It may be seen as a 1-D cross-section (along the positive $k_z$ **-axis)** of the dark shaded sphere in Figure 3. Note that $\omega_{max}$ has been chosen such that the spike in $\check{\Delta}'(k_z)$ just falls outside the area, occupied by the wavefield. Hence, following the reasoning above, the Born approximation does not account for the periodical variations in Figure 4a. This is confirmed in Figure 4c, which shows the exact reflection response and the result of the 1-D version of the Born approximation (6). Note that the Born approximation only contains the nondispersed response of the step at the primary traveltime $t_{prim}$ . It does not account for the time delay and dispersion caused by the fine layering. In principle, the time delay could be accounted for by choosing a slightly smaller value for the background velocity $\bar{c}$. However, the fact that the Born approximation does not account for the dispersion implies that in Born inversion this dispersion will blur the image of the step function.

**Nonlinear two-way representation**

The scattered field described by the Born approximation may be seen as the first term in the Neumann series (5). It appeared to be proportional to $\Delta(\mathbf{k}_D - \mathbf{k}_S)$**.** In a similar way it can be shown that the second term in the Neumann series is proportional to

$$\int_{\mathcal{R}^3} \frac{\check{\Delta}(\mathbf{k}_D - \mathbf{k})\check{\Delta}(\mathbf{k} - \mathbf{k}_S)}{|\mathbf{k}|^2 - \omega^2/\bar{c}^2}\, d^3\mathbf{k}. \tag{43}$$

Apparently, the entire function **i\(k)** contributes to $\{P(\mathbf{x})\}^{(2)}$. The same can be said about higher order approximations. In other words, the nonlinear, two-way representation *does* account for the small scale variations of $\Delta(\mathbf{x}')$. However, it cannot be expected that nonlinear, two-way inversion based on this representation converges for these small scale variations [since **b(k)** cannot be uniquely resolved from the integral in equation (43)]. As a matter of fact, to stabilize the nonlinear inversion in practice, the area outside the sphere in Figure 3 should be explicitly excluded from the inversion procedure (for instance by limiting the discretization of the medium to at most two samples per shortest wavelength). This also implies that nonlinear inversion does not account for the dispersion effects, such as illustrated in Figure 4c.

**Linearized one-way representation**

Consider the linearized one-way representation (27) (i.e., the one-way primary representation), applied to the limited scattering volume V. For the qualitative analysis, we replace the reflection operator $\hat{R}^+(\mathrm{x}')$ by a reflection coefficient $R^+(\mathrm{x}')$. For convenience, we define the propagators in a homogeneous macro model with velocity $\bar{c}$. Following the same reasoning as above, $\{P^-(\mathbf{x})\}^{(1)}$ is proportional to $\check{R}^+(\mathbf{k}_D - \mathbf{k}_S)$, where $R^+(\mathbf{k})$ represents the 3-D spatial Fourier transform of $R^+(\mathbf{x}')$ (see Figure 5). Hence, the linearized one-way representation and, consequently, wave-equation-based depth migration, do not account for the small scale variations of $R^+(\mathbf{x}')$, represented by the light shaded area in Figure 5.

**Generalized primary representation**

Similar as the two-way Neumann series (5), the one-way Bremmer series (28) does account for the effects of fine layering. However, for the same reasons as given above, the Bremmer series representation is not a good starting point for deriving a migration technique that compensates for the dispersion effects of tine layering.

As an alternative, consider the generalized primary representation (42), applied to the limited scattering volume V. It has been observed before that this representation accounts for all multiple scattering in V, hence, the angle-dependent dispersion effects related to the fine layering are included. As a matter of fact, they are included in the generalized primary propagators $W_g^+(\mathbf{x}', \mathbf{x}_S)$ and $W_g^-(\mathbf{x}, \mathbf{x}')$. For practical applications, these propagators may either be parameterized or they may be defined in an extended macro model that mimicks the effects of the fine layering (the medium parameters in such an extended macro model are complex valued and anisotropic, even when the actual medium parameters in the finely layered medium are real-valued and isotropic). In both cases, the fine layering is upscaled to macro parameters that are related to the statistics of the fine layering. For laterally invariant media, these two approaches are discussed, respectively, in Herrmann and Wapenaar (1993) and Wapenaar et al. (1994). For 3-D inhomogeneous media, these approaches are currently under investigation.

For the following qualitative analysis, we replace $\hat{R}^+(\mathbf{x}')$ again by $R^+(\mathbf{x}')$, and we assume for convenience that the propagators are defined in a homogeneous extended macro model. Then, based on the similarity between the primary representation (27) and the generalized primary representation (42), it follows that $P^-(\mathrm{x})$ is again proportional to $\check{R}^+(\mathbf{k}_D - \mathbf{k}_S)$ (the dark shaded sphere in Figure 5). The small scale variations of $R^+(\mathrm{x}')$ in equation (42), represented by the light shaded area in Figure 5, do not contribute to $P^-(x)$, hence, they may be removed by a 3-D spatial low-pass filter. This leads to the interesting observation that the generalized primary representation accounts for the effects of the fine layering, even when

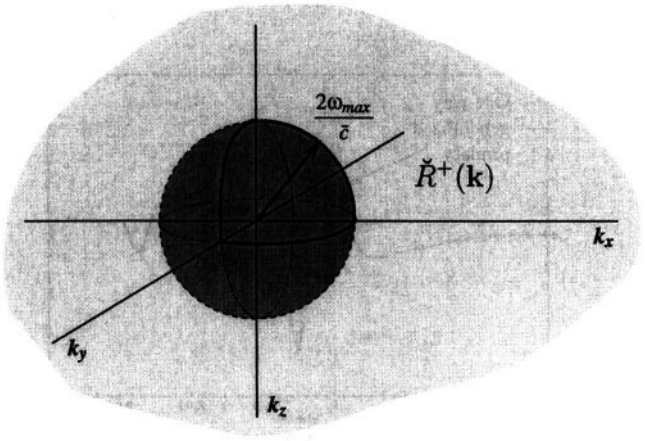


FIG. 5. Spatially Fourier transformed reflection function. The light shaded area, representative for the fine layering, does *not* contribute to the scattered wavefield, as described by the primary one-way representation.

1) $W_g^+(x', \mathbf{x}_S)$ and $W_g^-(x, x')$ are parameterized or defined in an extended macro model, and
2) $\hat{R}^+(x')$ in equation (42) is replaced by its low-pass filtered version.

Before we discuss the consequences for migration, we illustrate these two aspects for the laterally invariant medium introduced in Figure 4a. In both examples (Figures 6 and 7) the 1-D generalized primary propagators $W_g^+(z,0) = W_g^-(0,z)$ have been modeled according to $W_g^+(z,0) = \{W_g^+(z_1,0)\}^{z/z_1}$, where $W_g^+(z_1,0)$ is the exact (numerically modeled) transmission response at $zl$ = 1000 m. This is identical to defining the propagator in an extended homogeneous macro model, according to $W_g^+(z,0) = \exp(-j[\omega/\bar{c}(\omega)]z) = \{\exp(-j[\omega/\bar{c}(\omega)]z_1)\}^{z/z_1}$, where $\bar{c}(\omega)$ is a complex, frequency-dependent macro velocity. In the first example, the generalized primary response of the full reflection function (Figure 6a) is modeled, using the 1-D version of the generalized primary representation (42). The result is shown in Figure 6b, together with the exact response. Note that both responses fully overlap. In the second example, the reflection function is filtered by a spatial low-pass filter (Figure 7a). Using the same propagators as before, the response of this filtered reflection function appears again to be identical to the exact response, as is shown in Figure 7b. This confirms the observation made above.

The consequences for migration are the following. Of course, just as was the case for nonlinear, two-way inversion, migration cannot be expected to resolve the small scale variations of $\hat{R}^+(x')$, represented by the light shaded area in Figure 5. On the contrary, since the effects of the fine layering are included only in the propagators $W_g^+(\mathbf{x}', \mathbf{x}_S)$ and $W_g^-(x, x')$, it follows that the estimation of the fine layering should be integrated in "extended macro model estimation." Hence, apart from the main geological boundaries and average velocities, extended macro model estimation should aim for the parameters that characterize the statistics of the fine layering. Given the extended macro model, wave-equation- based depth migration may be formulated as a truly linear inversion of the generalized primary representation (42). The result is a true amplitude image of the reflection operator $\hat{R}^+(\mathbf{x}')$. This approach is discussed further in a companion paper (Wapenaar and Herrmann, 1996).

## REMARKS

As has been noted before, equation (38), and consequently, the generalized primary representation (42), are implicitly nonlinear in the scattering operator $\hat{\mathbf{\Theta}}$, i.e., in $\hat{R}^{\pm}$ and $\hat{T}^{\pm}$. However, the nonlinearities have been organized such that in their explicit form these representations are linear (not linear-

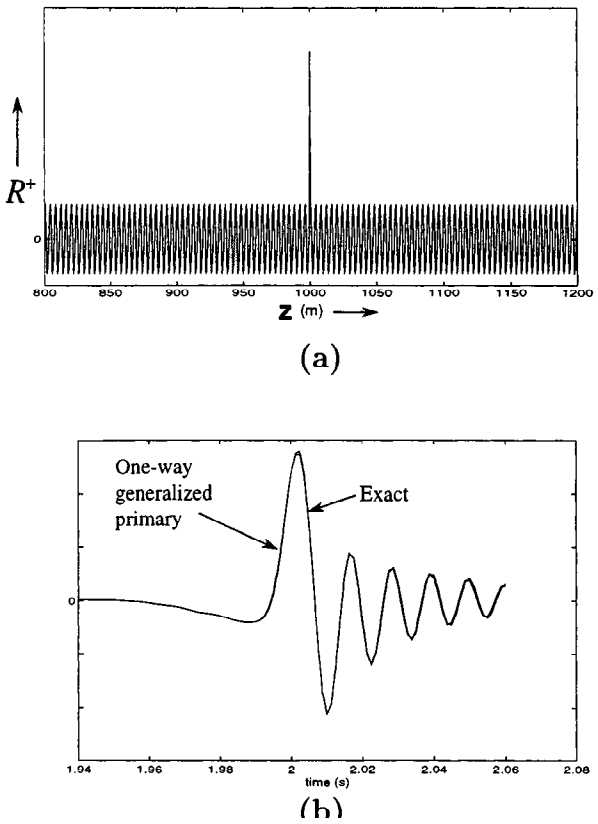


FIG. 6. 1-D illustration of the generalized primary representation. (a) Reflection function $R^+(z)$. (b) Reflection response according to the generalized primary representation.

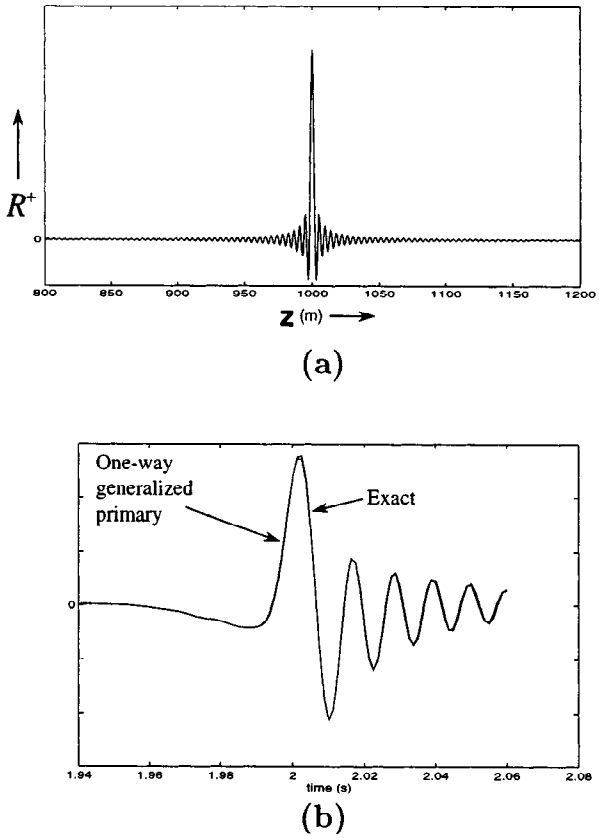


FIG. 7. 1-D illustration of the generalized primary representation. (a) Spatially filtered reflection function $\hat{R}^+(z)$. (b) Reflection response according to the generalized primary representation.

*ized!).* The scattering operators $\hat{R}^{\pm}$ and $\hat{T}^{\pm}$, that are implicitly present in $W_g^{\pm}$, play an entirely different role from $\hat{R}^{+}$(x') in the explicit representation (42). The former operators "modify" the primary waves between the surface and x'; the latter operator transforms the modified downgoing wave at x' into an upgoing wave. This explains why $\hat{R}^{\pm}$ in $W_g^{\pm}$ and $\hat{R}^{+}$(x') in equation (42) may be represented in two entirely different ways (i.e., statistical parameterization versus low-pass filtering), although they are actually the same operators. It also explains why there is no paradox for migration: imaging of the low-pass filtered version of $\hat{R}^{+}$(x') in equation (42) requires knowledge of only the *statistical* properties of $\hat{R}^{\pm}$ in $W_g^{\pm}$.

Note that the above discussed properties of the generalized primary representation are a consequence of the distinction between propagation and scattering in the operator matrix $\hat{\mathbf{B}} = -j\omega\hat{\mathbf{A}} + \hat{\Theta}$ in the one-way wave equation. The two-way wave equation does not make this distinction. For instance, suppose one would try to improve the linearized two-way representation (6) by defining G in an extended macro model, with complex valued $\bar{K}$ and $\bar{\varrho}$. Then by definition the contrast parameters $\Delta K$ and $\Delta\varrho$ would also become complex valued, which would give an undesired phase distortion. The reflection operator $\hat{R}^{+}$(x') in equation (42), on the other hand, is not affected by the choice of the extended macro model.

## CONCLUSIONS

Inversion aims at imaging the medium contrast parameters, whereas migration aims at imaging the vertical changes of the actual medium parameters (reflectivity). In this paper we have related inversion and migration to, respectively, two-way and one-way representations of the seismic data. The linearized one-way representation accounts more accurately for primary reflections than the linearized two-way representation. Hence, proper wave equation based depth migration produces more accurate results than linearized Born inversion. (This conclusion applies to the seismic situation, where the *boundaries* between the different layers are the main cause for scattering. It is not necessarily true for medical applications or NDT.)

The fine layering of the subsurface causes angle-dependent dispersion effects, that are generally ignored in inversion and migration. Although the two-way Neumann series and the one-way Bremmer series representations account for fine layering, they are not suitable starting points for deriving imaging techniques that compensate for the dispersion effects. Using the natural distinction between propagation and scattering in the one-way wave equation, we have introduced the 3-D generalized primary representation as an alternative for the one-way Bremmer series representation. In its explicit form, this representation is linear in the reflection operator; internal multiple scattering is implicitly included in the generalized primary propagators. An equivalent (mathematically consistent) two-way representation cannot be given.

Imaging based on the generalized primary representation involves:

1) Determination of an extended macro model (including the parameters that characterize the statistics of the fine layering)
2) True-amplitude (true AVA) migration by linear inversion of the generalized primary representation (42).

## ACKNOWLEDGMENT

The author thanks Dr. K. Pann and the anonymous reviewers for their constructive remarks and Mr. Reinoud Slot for generating the examples.

## REFERENCES

Berkhout, A. J., 1982, Seimic migration, Elsevier Science Publ. Co., Inc.
—, 1984, Multidimensional linearized inversion and seismic migration: Geophysics, 49, 1881-1895.
Berkhout, A. J., and Van Wulfften Palthe, D. W., 1979, Migration in terms of spatial deconvolution, Geophys. Prosp., 27, 261-291.
Berkhout, A. J., and Wapenaar, C. P. A., 1990, DELPHI: Delft philosophy on acoustic and elastic inversion, Part I: The Leading Edge, 9, No. 2, 30-33.
— 1993, A unified approach to acoustical reflection imaging. Part II: The inverse problem: J. Acoust. Soc. Am., 93, No. 4, 2017-2023.
Beydoun, W. B., Jin, S., and Hanitzsch, C., 1994, AVO migration and inversion: Are they commutable?: 64th Annual Internat. Mtg., Soc. Expl. Geophys., Expanded Abstracts, 952-955.
Bleistein, N., 1987, On the imaging of reflectors in the Earth: Geophysics, 52, 93 l-942.
Bleistem, N., and Cohen, J. K., 1982, Velocity inversion-Present status, new directions: Geophysics, 47, 1497-15 11.
Brekhovskikh, L. M., 1960, Waves in layered media: Academic Press, Inc.
Cheng, G., and Coen, S., 1984, The relationship between Born inversion and migration for common midpoint stacked data: Geophysics, 49, 2117-2131.
Claerbout, J. F., 1971, Toward a unified theory of reflector mapping (propagation): Geophysics, 36, 467-481.
— 1985, Imaging the Earth's interior: Blackwell Scientific Publications.
Clayton, R. W., and Stolt, R. H., 1981, A Born-WKBJ inversion method for acoustic reflection data: Geophysics, 46, 1559-1567.
Cohen, J. K., and Bleistein, N., 1979, Velocity inversion procedure for acoustic waves: Geophysics, 44, 1077-1087.
Corones, J., 1975, Bremmer series that correct parabolic approximations: J. Math. Anal. and Appl., 50, 361-372.
de Bruin, C. G. M., Wapenaar, C. P. A., and Berkhout, A. J., 1990, Angle-dependent reflectivity by means of prestack migration: Geophysics, 55, 1223-1234.
de Hoo , M. V., 1992, Directional decomposition of transient acoustic wave fields: Ph.D. thesis, Delft University of Technology.
Devaney, A. J., 1982, A filtered backpropagation algorithm for diffraction tomography: Ultrasonic Imaging, 4, 336 -350.
— 1984, Geophysical diffraction tomography: IEEE Trans. Geosci. Remote Sensing, GE-22, 3-13.
Fishman, L., McCoy, J. J., and Wales, S. C., 1987, Factorization and path integration of the Helmholtz equation: Numerical algorithms: J. Acoust. Soc. Am., 81, 1355-1376.
Herrmann, F. J., and Wapenaar, C. P. A., 1993, Wave propagation in finely layered media, a parametric approach: 63rd Ann. Internat. Mtg., Soc. Expl. Geophys., Expanded Abstracts, 909-912.
Hubral, P., 1983, Computing true amplitude reflections in a laterally inhomogeneous Earth: Geophysics, 48, 1051-1062.
Hubral, P., Treitel, S., and Gutowski, P. R., 1980, A sum autoregressive formula for the reflection response: Geophysics, 45, 1697-1705.
Kosloff, D. D., and Baysal, E., 1983, Migration with the full acoustic wave equation: Geophysics, 48, 677- 687.
Miller, D., Oristaglio, M., and Beylkin, G., 1987, A new slant on seismic imaging-Migration and integral geometry: Geophysics, 52, 943-964.
Morse, P. M., and Ingard, K. U., 1968, Theoretical acoustics: McGraw-Hill Book Co.
Raz, S., 1981, Three-dimensional velocity profile inversion from finite-offset scattering data: Geophysics, 46, 837-842.
Resnick, J. R., Lerche, I., and Shuey, R. T., 1986, Reflection, transmission, and the generalized primary wave: Geoph. J. Roy Astr. Soc., 87, 349-377.
Schneider, W. A., 1978, Integral formulation for migration in two and three dimensions: Geophysics, 43, 49 -76.
Schleicher, J., Tygel, M., and Hubral, P., 1993, 3-D true-amplitude, finite-offset migration: Geophysics, 58, 1112-l 126.
Stolt, R. H., 1978, Migration by Fourier transform: Geophysics, 43, 23-48.
Stolt, R. H., and Weglein, A. B., 1985, Migration and inversion of seismic data: Geophysics, 50, 2458 -2472.
Tarantola, A., 1984, Linearized inversion of seismic reflection data: Geophys. Prosp., 32, 998-1015.

Ursin, B., 1983, Review of elastic and electromagnetic wave propagation in horizontally layered media: Geophysics, 48, 1063-1081.
Wapenaar, C. P. A., 1996, One-way representations of seismic data: Geoph. J. Int., 127.
Wapenaar, C. P. A., and Berkhout, A. J., 1989, Elastic wavefield extrapolation: Elsevier Science Publ. Co., Inc.
Wapenaar, C. P. A., and Grimbergen, J. L. T., 1996, Reciprocity theorems for one-way wave fields: Geoph. J. Int., 127.
Wapenaar, C. P. A., and Herrmann, F. J., 1996, True-amplitude migration taking fine-layering into account: 61, 795-803.
Wapenaar, C. P. A., Slot, R. E., and Herrmann, F. J., 1994, Towards an extended macro model, that takes fine-layering into account: J. Seis. Expl., 3, 245-260.
Weglein, A. B., 1982, Multidimensional seismic analysis: Migration and inversion: Geoexpl., 20, 47-60.
Wolf, E., 1969, Three-dimensional structure determination of semi-transparent objects from holographic data: Optics Comm., 1, 153-156.
Wu, R. S., and Toksöz, M. N., 1987, Diffraction tomography and multisource holography applied to seismic imaging: Geophysics, 52, 1 l-25.